

Available online at www.sciencedirect.com



Nuclear Physics A 00 (2013) 1-4

Journal Logo

# Delineating the saturation boundary: linear vs non-linear QCD evolution from HERA data to LHC phenomenology

P. Quiroga-Arias<sup>a</sup>, J. L. Albacete<sup>b,c</sup>, J. G. Milhano<sup>d,e</sup>, J. Rojo<sup>e</sup>

<sup>a</sup>LPTHE, UPMC Univ. Paris 6 and CNRS UMR7589, Paris, France <sup>b</sup>IPNO, Université Paris-Sud, CNRS/IN2P3, F-91406, Orsay, France. <sup>c</sup>IPhT, CEA/Saclay, 91191 Gif-sur-Yvette cedex, France. <sup>d</sup>CENTRA, Instituto Superior Técnico, Universidade Técnica de Lisboa, Av. Rovisco Pais, P-1049-001 Lisboa, Portugal. <sup>e</sup>Physics Department, Theory Unit, CERN, CH-1211 Genève 23, Switzerland.

#### Abstract

The forthcoming p+Pb run at the LHC will provide crucial in formation on the initial state effects of heavy ion collisions and on the gluon saturation phenomena. In turn, most of the saturation inspired phenomenology in heavy ion collisions borrows substantial empiric information from the analysis of e+p data, where abundant high quality data on the small-x kinematic region is available. Indeed, the very precise combined HERA data provides a testing ground in which the relevance of novel QCD regimes, other than the successful linear DGLAP evolution, in small-x inclusive DIS data can be ascertained. We present a study of the dependence of the AAMQS fits, based on the running coupling BK non-linear evolution equations (rcBK), on the fitted dataset. This allows for the identification of the kinematical region where rcBK accurately describes the data, and thus for the determination of its applicability boundary. It also set important constraints to the saturation models used to model the early stages of heavy ion collisions. Finally we compare the rcBK results with NNLO DGLAP fits, obtained with the NNPDF methodology with analogous kinematical cuts. Further, we explore the impact on LHC phenomenology of applying stringent kinematical cuts to the low-x HERA data in a DGLAP fit.

## 1. Introduction: situation and strategy

The knowledge of the partonic structure of the proton at all relevant observation scales plays a crucial role in the analysis of data from present high-energy hadronic colliders, most notably at the LHC. There are different QCD approaches for the description of the scale dependence of parton distribution functions. The most commonly used framework are the DGLAP equations [1],

$$\frac{\partial f(x,Q^2)}{\partial \ln(Q^2/Q_0^2)} = \int_x^1 \frac{dy}{y} P\left(\alpha_s(Q^2), x/y\right) f(y,Q^2),$$
(1)

that have been successfully and intensively tested against experimental data. Successful as they are, the DGLAP equations are also expected to break down in some kinematic regimes, in particular at small values of Bjorken-*x*.

Analogous resummation schemes aimed at describing the small-x evolution of hadron structure, in the direction orthogonal in the kinematic plane to DGLAP evolution, have also been developed [2] (BFKL approach). Additionally, the enhancement of gluon emission at small-x naturally leads to the - empirically observed - presence of large gluon

Email address: pquiroga@lpthe.jussieu.fr (P. Quiroga-Arias)

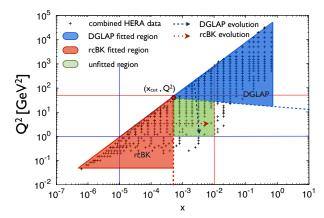


Figure 1. Sketch of the kinematic plane with cuts for DGLAP and rcBK fits. The arrows indicate backwards evolution in either formalism to the unfitted *test* region. This method provides a direct test of fit stability under changes in the boundary conditions.

densities and to the need of non-linear recombination terms in order to stabilize the diffusion towards the infrared characteristic of BFKL evolution. Both the resummation of small-*x* logarithms and the inclusion of non-linear density dependent corrections are consistently accounted for by the B-JIMWLK [3] equations. Its large-Nc limit, the BK equation, including running coupling corrections (henceforth referred to as rcBK)

$$\frac{\partial \mathcal{N}(r,x)}{\partial \ln(x_0/x)} = \int d^2 r_1 \mathcal{K}(r,r_1,r_2) \left[ \mathcal{N}(r_1,x) + \mathcal{N}(r_2,x) - \mathcal{N}(r,x) - \mathcal{N}(r_1,x)\mathcal{N}(r_2,x) \right],$$
(2)

was shown in [4] to be compatible with experimental data from different collision systems (confirmed in [5]).

Based on theoretical arguments alone, one can only strictly establish the applicability of either DGLAP or rcBK in their asymptotic limits of very large  $Q^2$  or very small *x* respectively. On the phenomenological side, where intermediate  $(x,Q^2)$  kinematics is probed, the situation remains unclear. Thus, one needs to define some suitable strategy to identify the regimes of validity of each formalism and quantify the potential deviation from these [6], and this is precisely what we intend to do in the work presented in this proceedings.

The strategy to search for statistically significant deviations from DGLAP evolution was laid down in [7], where subsets of data on the reduced DIS cross section  $\sigma_r(x, Q^2)$  measured at HERA [8], were excluded from the fitted data set below some given kinematic cuts  $Q^2 \leq Q_{cut}^2 \equiv A_{cut} x^{-\lambda}$ , with  $\lambda \sim 0.3$  and different values of  $A_{cut}$ , inspired by the generic expectation that possible deviations from fixed order DGLAP are larger at small-*x* and  $Q^2$ . The PDFs were fitted only in the safe kinematical region of the approach, and then backwards DGLAP evolution was used to compare with the excluded, potentially troublesome, data. The analysis of [7] found a systematic discrepancy, albeit with not large enough statistical significance for a decisive statement to be made, indicating that additional dynamics may play a role in the parton evolution in the unfitted region.

Following an analogous procedure, we perform fits to data based on the rcBK non-linear evolution equations, limiting the data sets fitted to the safe region of the approach (low-*x* and  $Q^2$ ), and then study the stability of the fits with respect to the choice of datasets. We systematically reduce the largest experimental value of *x* included in the fit,  $x_{\text{cut}}$ , and then use the resulting parametrization for the dipole scattering amplitude<sup>1</sup> to predict the value of  $\sigma_r(x, Q^2)$  in the unfitted region  $x_{\text{cut}} < x < x_0$ . Fig. 1 summarizes the fitting strategy for the analyses with kinematical cuts.

## 2. Results: rcBK (AAMQS) and NNLO DGLAP (NNPDF)

We now show the results with various kinematical cuts obtained with rcBK and DGLAP evolution equations. Fig. 2-left shows the comparison of the theoretical results stemming from rcBK fits to data with different *x*-cuts from

<sup>&</sup>lt;sup>1</sup>See [9] for a detailed explanation of the AAMQS implementation of the rcBK evolution, and [6] for details on the method.

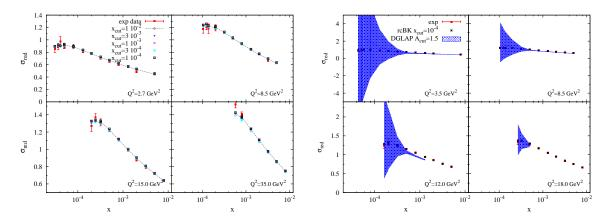


Figure 2. (*left*) Comparison of the result for reduced cross section obtained with rcBK fits with different cuts and HERA data for four different bins in  $Q^2$ . (*right*) rcBK cut fit with  $x_{cut} = 10^{-4}$  and the DGLAP fit with  $A_{cut} = 1.5$ , compared to the experimental HERA-I data. The comparison is shown in four different bins in  $Q^2$ . In the DGLAP case the band corresponds to the PDF uncertainties.

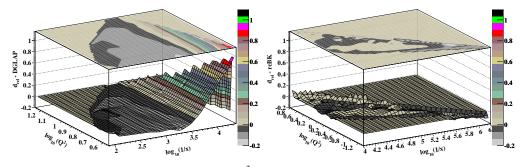


Figure 3. The relative distance,  $d_{rel}(x, Q^2)$ , for DGLAP (left) and rcBK (right) cut fits.

 $x_{\text{cut}} = 10^{-2}$  to  $10^{-4}$ . The quality of the fits is comparably good independently of the cut, despite the decreasing number of points with decreasing  $x_{\text{cut}}$ . Also the extrapolations of the results for  $\sigma_r$  from fits with cuts to the unfitted region, i.e to  $x > x_{\text{cut}}$ , yield a good description of the data. Fig. 2-right shows the results corresponding to the rcBK fit with the most stringent cut,  $x_{\text{cut}} = 10^{-4}$ , together with experimental data and the analogous results from the NNLO DGLAP fit with cut  $A_{\text{cut}} = 1.5$ . While the DGLAP extrapolations to the unfitted, *test* region are compatible with data within the uncertainty bands, the central values of the predictions show significant deviations from data in the region of small-x.

We quantify these deviations by calculating the relative distance between the theoretical results and experimental data,  $d_{rel}(x, Q^2) = \frac{\sigma_{r,th} - \sigma_{r,exp}}{(\sigma_{r,th} + \sigma_{r,exp})/2}$ , both for the rcBK and DGLAP cut fits, with cut values  $x_{cut} = 10^{-4}$  and  $A_{cut} = 1.5$  respectively. As shown in Fig. 3,  $d_{rel}$  is on average much smaller for the rcBK fits than it is for the DGLAP one, the latter also showing a systematic trend to underestimate data at small-*x* and to overshoot them at larger *x*. In turn, the rcBK values for  $d_{rel}$  alternate in sign in all the unfitted region.

In order to explore the predictive power of the rcBK approach and the sensitivity to boundary effects encoded in the different initial conditions for the evolution under the inclusion/exclusion of subsets of data we extrapolate our results for the total  $F_2(x, Q^2)$  and longitudinal  $F_L(x, Q^2)$  structure functions to values of x smaller than those currently available experimentally. The results, Fig. 4, show that the predictions stemming from different fits converge, within approximately one percent accuracy, at values of  $x \sim 10^{-4}$ . These predictions could be verified in planned facilities as the LHeC [10] or the EIC [11], where a much extended kinematic reach in x would be available

To conclude, we need to explore the impact that potential deviations from DGLAP evolution may have on LHC phenomenology. We compute benchmark LHC cross sections with the PDF sets both with and without the small-x kinematical cuts using the NNPDF2.1 NNLO set. The results are shown in Fig. 5. While the impact of cutting the small-x and small- $Q^2$  HERA data from the fit is rather moderate at LHC 7 TeV, at LHC 14 TeV the effect is much

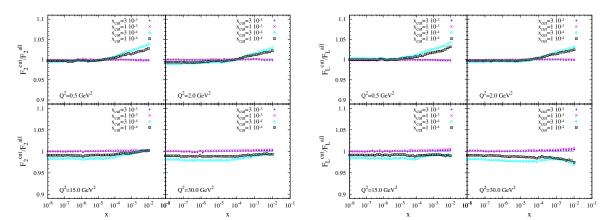


Figure 4. Extrapolation to the low-x region from the rcBK cut fits presented in Fig. 2. The total,  $F_2(x, Q^2)$  (*left*), and longitufinal,  $F_L(x, Q^2)$  (*right*), structure functions are calculated down to  $x = 10^{-8}$ . The results are presented as a ratio of the prediction for the different cut fits to the prediction for the uncut fit, i.e. a fit to all data with  $x < x_0 = 10^{-2}$  and  $Q^2 < 50$  GeV<sup>2</sup>.

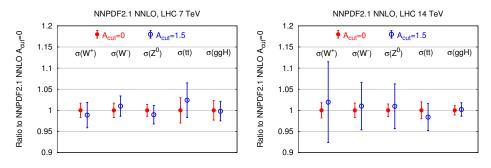


Figure 5. Comparison of the predictions for LHC NNLO cross sections for the reference NNPDF2.1 NNLO fit with  $A_{cut} = 0$  and with the NNPDF2.1 NNLO fit with  $A_{cut} = 1.5$ . Cross sections are shown as ratios to the uncut  $A_{cut} = 0$  predictions. We show results both for LHC 7 TeV (left plot) and for LHC 14 TeV (right plot).

larger, since smaller values of x in the PDFs are being probed. One can observe that the cross section for Higgs boson production in gluon fusion is very stable against the kinematical cuts, while for the electroweak boson and top production cross sections the PDF uncertainties increase by up to a factor five. This needs to be carefully considered, since these processes constitute an important background in Higgs searches.

#### References

- Y.L. Dokshitzer, Sov. Phys. JETP 46 (1977) 641. V.N. Gribov and L.N. Lipatov, Sov. J. Nucl. Phys. 15 (1972) 438. G. Altarelli and G. Parisi, Nucl. Phys. B126 (1977) 298.
- [2] E.A. Kuraev, L.N. Lipatov and V.S. Fadin, Sov. Phys. JETP 45 (1977) 199. I. Balitsky and L. Lipatov, Sov.J.Nucl.Phys. 28 (1978) 822.
- [3] I. Balitsky, Nucl. Phys. B463 (1996) 99, hep-ph/9509348. Y.V. Kovchegov, Phys. Rev. D60 (1999) 034008, hep-ph/9901281. J. Jalilian-Marian et al., Phys. Rev. D59 (1998) 014014, hep-ph/9706377. A. Kovner, J.G. Milhano and H. Weigert, Phys. Rev. D62 (2000) 114005, hep-ph/0004014. H. Weigert, Nucl. Phys. A703 (2002) 823, hep-ph/0004044.
- [4] J.L. Albacete and Y.V. Kovchegov, Phys. Rev. D75 (2007) 125021, arXiv:0704.0612 [hep-ph].
- [5] J.L. Albacete et al., Phys. Rev. D80 (2009) 034031, arXiv:0902.1112.
- [6] J. L. Albacete, J. G. Milhano, P. Quiroga-Arias and J. Rojo, arXiv:1203.1043 [hep-ph].
- [7] F. Caola, S. Forte and J. Rojo, Phys. Lett. B686 (2010) 127, arXiv:0910.3143. F. Caola, S. Forte and J. Rojo, Nucl.Phys. A854 (2011) 32, arXiv:1007.5405.
- [8] H1, F.D. Aaron et al., JHEP 01 (2010) 109, arXiv:0911.0884.
- [9] J.L. Albacete et al., Eur.Phys.J. C71 (2011) 1705, arXiv:1012.4408.
- [10] M. Klein et. al., EPAC'08, 11th European Particle Accelerator Conference (2008).
- [11] The Electron Ion Collider: A white paper, BNL Report BNL-68933-02/07-REV, Eds. A. Deshpande, R. Milner and R. Venugopalan. .